Title

Mutations in the miRNA165/166 binding site of the HB2 gene result in pleiotropic effects on morphological traits in wheat

Journal

The Crop Journal, 11(1)

ISSN

2095-5421

Authors

Jiang, Dengji
Hua, Lei
Zhang, Chaozhong
et al.

Publication Date

2023-02-01

DOI

10.1016/j.cj.2022.05.002

Peer reviewed

The Crop Journal xxx (xxxx) xxx

Contents lists available at ScienceDirect

The Crop Journal

journal homepage: www.keaipublishing.com/en/journals/the-crop-journal/

Mutations in the miRNA165/166 binding site of the *HB2* gene result in pleiotropic effects on morphological traits in wheat

Dengji Jiang [a,1], Lei Hua [a,1], Chaozhong Zhang [b,1], Hongna Li [a], Zheng Wang [a], Jian Li [a], Guiping Wang [a], Rui Song [a], Tao Shen [a], Hongyu Li [a], Shengsheng Bai [a], Yanna Liu [a], Jian Wang [a], Hao Li [c], Jorge Dubcovsky [b], Shisheng Chen [a,*]

[a] *Peking University Institute of Advanced Agricultural Sciences, Weifang 261000, Shandong, China*
[b] *Department of Plant Sciences, University of California, Davis, CA 95616, USA*
[c] *State Key Laboratory of Crop Stress Adaptation and Improvement, College of Agriculture, Henan University, Kaifeng 475004, Henan, China*

ARTICLE INFO

Article history:
Received 27 April 2022
Revised 29 April 2022
Accepted 18 May 2022
Available online xxxx

Keywords:
Wheat
miRNA165/166
Curled leaves
Paired spikelets
Homeodomain-leucine zipper transcription factor

ABSTRACT

Leaf, spike, stem, and root morphologies are key factors that determine crop growth, development, and productivity. Multiple genes that control these morphological traits have been identified in Arabidopsis, rice, maize, and other plant species. However, little is known about the genomic regions and genes associated with morphological traits in wheat. Here, we identified the ethyl methanesulfonate-derived mutant wheat line M133 that displays multiple morphological changes that include upward-curled leaves, paired spikelets, dwarfism, and delayed heading. Using bulked segregant RNA sequencing (BSR-seq) and a high-resolution genetic map, we identified *TraesCS1D02G155200* (*HB-D2*) as a potential candidate gene. *HB-D2* encodes a class III homeodomain-leucine zipper (HD-ZIP III) transcription factor, and the mutation was located in the miRNA165/166 complementary site, resulting in a resistant allele designated *rHb-D2*. The relative expression of *rHb2* in the mutant plants was significantly higher ($P < 0.01$) than in plants homozygous for the WT allele. Independent resistant mutations that disrupt the miRNA165/166 complementary sites in the A- (*rHb-A2*) and B-genome (*rHb-B2*) homoeologs showed similar phenotypic alterations, but the relative intensity of the effects was different. Transgenic plants expressing *rHb-D2* gene driven by the maize *UBIQUITIN* (UBI) promoter showed similar phenotypes to the *rHb-D2* mutant. These results confirmed that *HB-D2* is the causal gene responsible for the mutant phenotypes. Finally, a survey of 1397 wheat accessions showed that the complementary sites for miRNA165/166 in all three *HB2* homoeologs are highly conserved. Our results suggest that *HB2* plays an important role in regulating growth and development in wheat.

1. Introduction

Bread or common wheat (*Triticum aestivum*; AABBDD genomes) is one of the most important cereal crops in terms of both cultivated area and total production (FAOSTAT, https://www.fao.org/faostat/en/), and it plays a key role as a staple food for much of the world's human population. Common wheat has undergone two recent allopolyploidization events, and as a result, the inheritance of morphological traits in wheat tends to be complex and quantitative [1]. In addition, the large (approximately 17 Gb) and complex nature of the hexaploid wheat genome has limited in-depth genetic studies of morphological traits.

Leaf, spike, stem, and root morphologies (henceforth referred to as plant architecture) are agriculturally important traits that have been extensively studied in Arabidopsis (*Arabidopsis thaliana*), rice (*Oryza sativa*), maize (*Zea mays*) and other plant species [2–4] because of their potential large effects on development and productivity. Scientists have expended considerable effort to identify the key genes that control multiple morphological changes, and thus, some genes related to plant architecture have been identified. In Arabidopsis, the *REVOLUTA* (*REV*) gene is necessary for apical meristem development and for limiting cell divisions in the stems and leaves [2]. In rice, plants with a mutation in the miRNA165/166 target sequence of the transcription factor *lateral florets 1* (*lf1*) show three-floret spikelet and rolled-leaf phenotypes

* Corresponding author.
E-mail address: shisheng.chen@pku-iaas.edu.cn (S. Chen).
[1] These authors contributed equally to this work.

https://doi.org/10.1016/j.cj.2022.05.002

[3,5]. Defects in the genes *narrow leaf and dwarf 1* (*ND1*), *curled and dwarf leaf 1* (*OsCD1*), and *narrow and rolled leaf 1* (*OsCslD4*) result in dwarfed plants with narrow and curled leaves [6–8]. In maize, *rolled leaf1* (*rld1*) encodes a homeodomain leucine zipper class III (HD-ZIP III) protein that controls the upward rolling of the leaf blade [4].

Previous studies have shown that HD-ZIP III transcription factors play important roles in the embryo [9], spike [3], root [10], and shoot and leaf development [11]. It is well documented that HD-ZIP III members are regulated by miRNA165/166 and are required for vascular development, shoot apical meristem (SAM) establishment, and polarity formation in lateral organs [12,13]. The HD-Zip III family in Arabidopsis contains five genes: *REVOLUTA* (*REV*), *PHABULOSA* (*PHB*), *CORONA* (*CNA*), *PHAVOLUTA* (*PHV*), and *ATHB8* [14]. These genes have redundant or antagonistic roles in Arabidopsis development [11]. The HD-Zip III family in rice also consists of five members, including *OsHox10*, *OsHox9*, *OsHox33*, *OsHox32*, and *OsHox29* (also named *OsHB1* to *OsHB5*) [15]. In contrast, there are few studies in wheat on the identification of genomic regions/genes involved in determining plant architecture.

In the present study, we identified and characterized a mutant line, M133, derived from an EMS-mutagenized population of the wheat cultivar 'Ningchun 4' [16]. M133 displayed multiple morphological changes, such as upward-curled leaves, paired spikelets, dwarfism, and delayed heading. A single genetic locus, temporarily designated as *Abnormal Plant Architecture-1* (*APA1*), was found to be responsible for the mutant phenotypes. The objectives of this study were to: (1) characterize and genetically map *APA1*; (2) identify potential candidate genes in the sequenced wheat genome; and (3) validate candidate genes using independent EMS mutants and transgenic plants.

2. Materials and methods

2.1. Plant materials and mapping population

An EMS-mutagenized population of the hexaploid Chinese wheat variety 'Ningchun 4' (NC4) was previously developed to clone the male sterility gene *MS1* [16]. The initial screen of this EMS mutant population was carried out in the 2009–2010 growing season. We identified an M_2 mutant line (M133) displaying upward-curled leaves, paired spikelets, dwarfism, delayed heading, and decreased fertility. Subsequently, this mutant (M_3 generation) was grown in a growth chamber environment (25 °C day/23 °C night; 18 h light/6 h dark photoperiod), and it was stably inherited through two generations of self-pollination. To genetically characterize this mutant line, M_5-generation individuals were crossed with the wild-type NC4, generating an F_2 population comprised of 168 individuals. To eliminate the influence of background mutations, we generated another BC_2F_2 population consisting of 500 individuals. Phenotypic data from the F_1, F_2, $F_{2:3}$, and BC_2F_2 populations was used to map the causal gene. The $F_{2:3}$ families were sown in one-meter-long rows (~25 seeds per family) in the field at Peking University Institute of Advanced Agricultural Sciences, Weifang, Shandong province, China (36°26′04.0″N, 119°26′42.6″E).

2.2. Bulked segregant analysis-RNA-Seq (BSR-seq)

Based on the phenotypic information, 15 homozygous wild-type and 15 homozygous mutant $F_{2:3}$ families were grown at 25 °C day/23 °C night with an 18 h light/6 h dark photoperiod for 14 days, and pooled tissues were collected to construct the wild-type bulk (W-bulk) and mutant bulk (M-bulk) for RNA extraction. Total RNA of the parents and bulks was extracted using the Spectrum Plant Total RNA Kit (MilliporeSigma, St. Louis, MO, USA). RNA-seq was performed on an Illumina HiSeq 4000 platform at Beijing Novogene Bioinformatics Technology Co., Ltd. (Beijing, China). Raw sequencing reads were trimmed using the software Trimmomatic v 0.32 [17] to remove low-quality reads and adaptors. Trimmed reads were aligned to the published reference genome of the hexaploid wheat 'Chinese Spring' (CS) RefSeq v1.1 [18] using the software STAR version 2.5.0c [19]. Variant calling was carried out using the HaplotypeCaller tool from GATK v3.2–2 [20]. The single nucleotide polymorphism (SNP)-index and Δ (SNP-index) [21,22] were calculated to identify candidate genomic regions.

2.3. Marker development

SNPs associated with the *APA1* locus were identified by BSR-seq analysis and were selected for the development of Kompetitive Allele-Specific Polymerase Chain Reaction (KASP) or Cleaved Amplified Polymorphic Sequence (CAPS) markers. The methods and procedures for developing KASP and CAPS markers have been reported previously [23,24]. The sequences flanking the target SNPs were obtained from the 'Chinese Spring' reference genome [18]. Genome-specific primers were developed using the software Primer3 web version 4.1.0 (https://primer3.ut.ee/) to amplify gene regions containing the target SNPs. NEBcutter v3.0.15 (https://nc3.neb.com/NEBcutter/) was used to determine the restriction enzymes that selectively cut the sequences containing the targeted SNPs. To obtain more SNPs between NC4 and the mutant line M133, we aligned the NC4 and M133 sequences from the RNA-seq data, identified polymorphisms, and generated markers within the candidate gene region.

2.4. Phylogenetic analysis

After searching the sequenced genomes of rice (*Oryza sativa*, https://www.ricedata.cn/gene/), maize (*Zea mays*, https://maizegdb.org/), barley (*Hordeum vulgare*, https://plants.ensembl.org/Hordeum_vulgare/Info/Index), *Brachypodium* (https://phytozome-next.jgi.doe.gov/), *Aegilops tauschii* (https://plants.ensembl.org/Aegilops_tauschii/Info/Index), and the hexaploid wheat variety 'Chinese Spring' (https://wheat-urgi.versailles.inra.fr/Seq-Repository/BLAST) using the sequences of HD-Zip III proteins from Arabidopsis as queries, we obtained 43 protein sequences for phylogenetic analysis. All protein sequences were aligned with Muscle as implemented in the software package MEGA version 7 [25], and phylogenetic trees were then produced using the Neighbor-Joining method. Finally, the software Interactive Tree Of Life (iTOL) v.5 was used to visualize the phylogenetic tree (https://itol.embl.de/).

2.5. Quantitative reverse transcription PCR (qPCR) analysis

Plants were grown in growth chambers with the following temperature and photoperiod: 25 °C day/23 °C night, 18 h light and 6 h dark. Leaves and roots were collected from BC_2F_3 sister lines at the two-leaf stage. Young spikes (~10 mm) and stems were sampled at later stages. Total RNA was isolated individually from different wheat tissues (leaf, stem, root, and spike) using the Spectrum Plant Total RNA Kit (MilliporeSigma). RNA samples were purified using the Direct-zol RNA MiniPrep Plus kit (Zymo Research, Irvine, CA, USA). To eliminate DNA contamination, we performed the on-column RNase-Free DNase I digestion following the manufacturer's instructions. After examining the integrity of the RNA samples, the concentrations were determined using a NanoDrop OneC spectrophotometer (Thermo Fisher Scientific, Waltham, MA, USA).

First-strand complementary DNA (cDNA) was synthesized from 1 μg of total RNA using ProtoScript II First Strand cDNA Synthesis

Kit (New England Biolabs, Hitchin, UK). qPCR reactions were performed on an ABI QuantStudio 5 Real-Time PCR System (Applied Biosystems, Foster City, CA, USA) with PowerUp SYBR Green Master Mix (Thermo Fisher Scientific). The *ACTIN* gene was used as the endogenous control for normalization of gene expression [26]. Transcript levels were presented as fold-*ACTIN* levels using the $2^{-\Delta CT}$ method as described previously [27].

2.6. EMS mutants

The sequenced EMS mutagenized populations of the hexaploid cultivar 'Cadenza' [28] are available on line (https://www.wheat-tilling.com/). Another sequenced EMS mutagenized population of the Chinese hexaploid cultivar 'Jimai 22' (https://jm.ytjebc.com/) was also used in this study. We screened these two databases for mutations using BLASTN with the sequences of *TraesCS1D02G155200*, *TraesCS1A02G157500*, and *TraesCS1B02G173900* as search queries. The plants from the selected 'Cadenza' mutant lines were grown in a greenhouse at the University of California, Davis (CA, USA).

2.7. Energy of miRNA165/166-target interaction

The predicted energy of the interactions between miRNA165/166 and the target sites were determined using the RNAhybrid on line tool [29]. For this analysis, we used the miRNA165/166 mature sequence and as targets the wild type *HB2* and the mutant alleles M133, Cadenza1761 and Cadenza0269, including 12 nt at each side, which are conserved in the three homoeologs.

2.8. Wheat transformation

We amplified the coding region of the candidate gene from the mutant line M133 using PrimeSTAR Max DNA Polymerase (TaKaRa, Tokyo, Japan), and generated the DNA construct for plant transformation in the binary vector pCAMBIA1300. The primer pair *HB-CD647* was used to amplify the *rHb-D2* coding region (Table S1). The amplified PCR product was gel purified using the NucleoSpin Gel and PCR Clean-up kit (Macherey-Nagel, Germany) and recombined into the linearized pCAMBIA1300 vector using the In-Fusion HD Cloning Kit (Clontech, Mountain View, CA, USA) following the manufacturer's instructions. The construct pCAMBIA1300-*rHb-D2* contained the maize *UBIQUITIN* (UBI) promoter fused to the amplified *rHb-D2* coding region (2517 bp), hereafter referred to as UBI:-*rHb-D2*. The resulting plasmid was transformed into the hexaploid wheat variety 'Fielder' using *Agrobacterium tumefaciens* strain EHA105-mediated transformation at the Peking University Institute of Advanced Agricultural Sciences transformation facility. The primer pair *HB-JCX* developed from the *rHb-D2* sequence was used to confirm the presence of the transgene in potential transgenic plants.

2.9. Allelic variation

The published reference genomes of diploid [30,31], tetraploid [32,33] and hexaploid [34,35] wheat varieties were used to detect allelic variations in the *HB2* candidate gene. In addition, we also used exome-capture data from three wheat panels to study variations in the *HB* candidate gene. The three wheat panels consist of 811 (after imputation and filtering) [36], 512 [37], and 59 wheat accessions [38], respectively.

3. Results

3.1. Characterization of the EMS-derived wheat mutant line M133

Based on the phenotyping data, M_5 plants of the mutant line M133 (*apa1*) exhibited multiple phenotypic changes including upward-curled leaves, paired spikelets, and dwarfism, when compared to the wild-type (WT) control plants (Fig. 1). To study this mutant line further, we performed a genetic analysis using F_1, F_2, and $F_{2:3}$ populations from the cross NC4 × M133. We first evaluated the rolled-leaf phenotype, which is a prominent feature of the mutant plants (Fig. 1B, D). We observed that the F_1 plants derived from crossing the parental lines showed an intermediate phenotype (Figs. 1D, S1). Among the 168 F_2 plants and their corresponding $F_{2:3}$ families, 42 families showed the homozygous rolled-leaf phenotype, 88 were segregating, and 38 were homozygous for the normal WT leaf phenotype, which fits the 1:2:1 segregation ratio expected for a single genetic locus ($\chi^2 = 0.57$, $P = 0.75$).

In the same F_2 and $F_{2:3}$ populations, we also investigated plant height and paired spikelets, which also segregated and showed obvious phenotypic differences (Fig. 1C, E). The data showed that the rolled-leaf phenotype is completely linked with the plant height and paired spikelet phenotypes, indicating that they may be controlled by the same gene. To reduce potential variability derived from background mutations, we crossed M133 mutant plants with WT NC4 and then backcrossed two times to NC4. The BC_2F_1 plants were self-pollinated and a BC_2F_2 population consisting of 500 individuals was generated. In this population, we investigated multiple agronomic traits, including rolled leaves, plant height, and paired spikelets, and found that these traits were significantly correlated with each other ($P < 0.001$). In addition, we observed that the fertility of the homozygous mutant plants in both F_2 and BC_2F_2 populations was greatly reduced ($P < 0.001$) when plants were grown at 25 °C day/23 °C night with an 18 h light/6 h dark photoperiod.

3.2. Validation of the phenotypic changes using BC_2F_3 sister lines

We selected BC_2F_3 sister lines homozygous for the WT and mutant alleles to further determine the phenotypic changes. At maturity, BC_2F_3 plants homozygous for the mutant allele showed a significant reduction in leaf width (49.6%) and length (31.8%) relative to those homozygous for the WT allele (Fig. 2A, B). The main stems in the BC_2F_3 mutant plants were significantly shorter than in the WT sister lines ($P < 0.0001$; Fig. 2C). The reduced stem length was associated with decreases in the length of the third, fourth, and fifth internode by 28.5%, 52.4%, and 75.1%, respectively, while the lengths of the first and second internode were not significantly different (Fig. 2D). For spike morphological traits, in addition to the BC_2F_3 plants homozygous for the WT and mutant alleles, we measured heterozygous BC_2F_3 plants because they also showed paired spikelets (Fig. 1E). We observed that the plants carrying the mutant alleles displayed abnormal spikes (Fig. 1E) where the awns and spikes were trapped in the rolled leaves. There was no significant difference in the average number of primary spikelets per spike among the three allelic classes (Fig. 2E). However, we found that the heterozygous and homozygous mutant BC_2F_3 plants had an average of 8.1 and 11.5 secondary spikelets (paired spikelets), which were not observed in the WT sister line ($P < 0.0001$; Fig. 2F). There was no significant difference in spike length between the WT and heterozygous plants, but spikes from plants homozygous for the mutant allele were significantly shorter ($P < 0.0001$; Fig. 2G). Finally, we examined 6-day-old wheat seedlings (Fig. 1F) and found a decrease in the number of seminal roots (6.8%, $P < 0.05$; Fig. 2H) and length of the primary roots (12.9%,

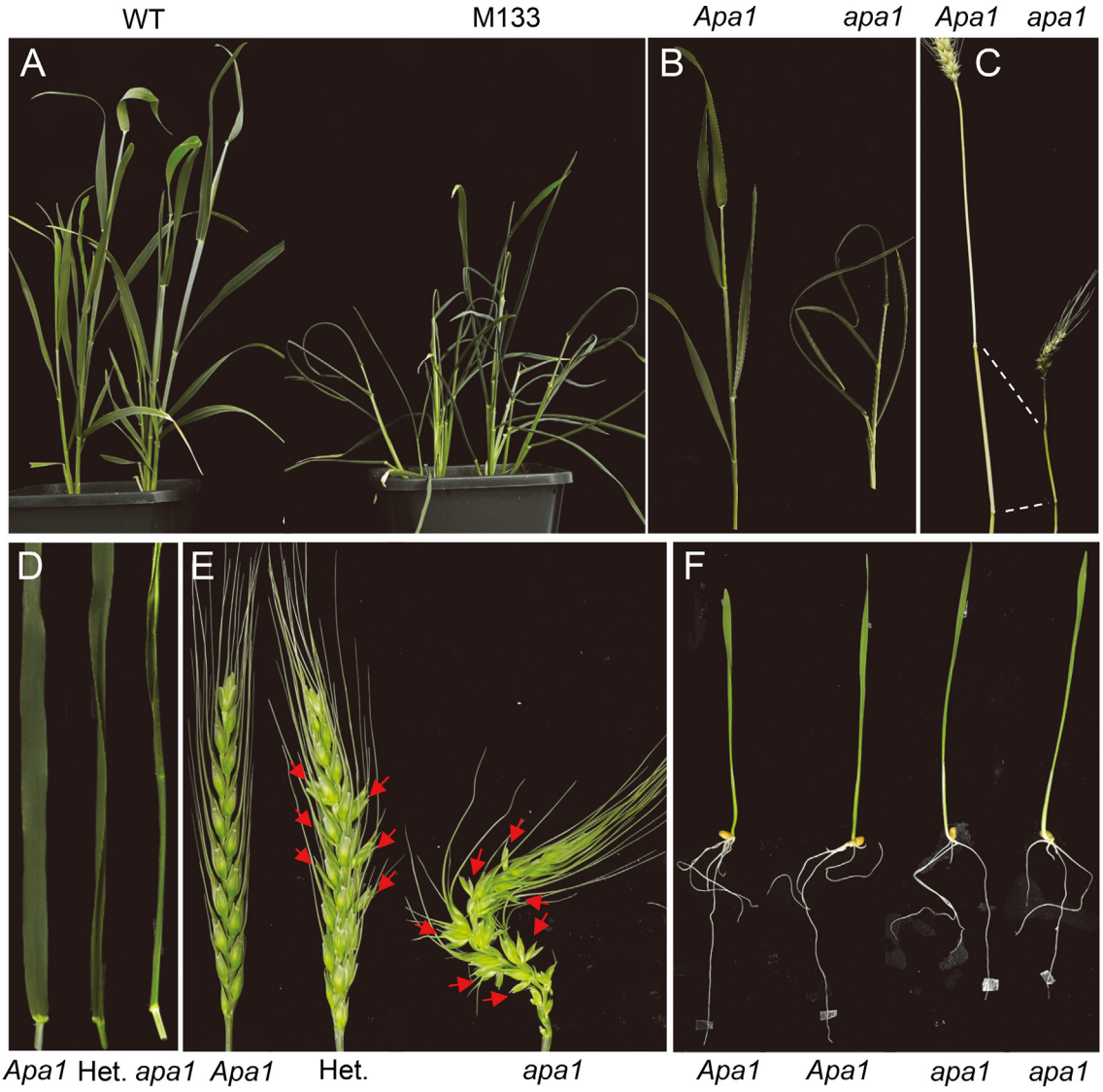

Fig. 1. Phenotypic changes in M133 mutant plants. (A) WT and M133 plants grown in a controlled environment. (B) Close-up views of the main tillers. (C) A close-up of the internodes. Dashed white lines represent the positions of the nodes. (D) The rolled-leaf phenotype in BC_2F_3 plants homozygous for *Apa1* and *apa1* and heterozygous plants. (E) Spike phenotypes (red arrows indicate paired spikelets). (F) Root phenotypes (6-day-old seedlings). Plants were grown at 25 °C day/23 °C night with an 18 h light/6 h dark photoperiod. WT, wild type; *Apa1*, BC_2F_3 plants homozygous for the WT allele; *apa1*, BC_2F_3 plants homozygous for the mutant allele; Het., heterozygous (*Apa1*/*apa1*) BC_2F_3 plants.

$P < 0.05$; Fig. 2I) in the BC_2F_3 plants homozygous for the mutant allele relative to those homozygous for the WT allele.

When BC_2F_3 plants carrying the WT and mutant alleles were grown at 25 °C day/23 °C night with an 18 h light/6 h dark photoperiod, we observed that BC_2F_3 plants carrying the mutant allele flowered 2.3 days later than those carrying the WT allele ($P < 0.01$, Fig. S2). To further confirm this result, we performed another experiment at a lower temperature with a shorter photoperiod (10 °C/12 h light and 12 h dark). Statistical analyses showed that BC_2F_3 plants homozygous for the mutant allele headed 8.8 days later ($P < 0.0001$) than those carrying the WT allele under these conditions (Fig. S3), a larger delay than in the previous 25 °C day/23 °C night long-day experiment. Using the 168 $F_{2:3}$ families described above, we confirmed that heading time was linked to the other phenotypic changes. In addition, we found that the intensity of the morphological defects in the stem and leaf organs (rolled leaf and dwarfism) in the BC_2F_3 mutant plants was weaker when plants were grown at 12 h light/10 °C than when grown at 18 h light/25 °C day/23 °C night (Fig. S3A, B). This result suggests that some of the phenotypic defects in mutant plants may be sensitive to photoperiod or/and temperature. Taken together, these multiple linked mutant phenotypes indicate that the M133 mutated gene has multiple effects on wheat growth and development.

3.3. Genetic mapping of a locus on chromosome 1D by BSR-seq

To map the causal gene, we carried out bulked segregant RNA-seq (BSR-seq) on an $F_{2:3}$ mapping population derived from the cross of NC4 × M133. RNA sequencing reactions generated, on average, 50.1 million 150-base raw read pairs per sample (NCBI SRA database accession number PRJNA826248; NC4, M133, W-bulk, and M-bulk). After trimming the reads and filtering them for quality and adapter contamination, ~99% of the reads remained and were aligned to the 'Chinese Spring' wheat reference genome RefSeq v1.1. Approximately 82% of the filtered read pairs mapped uniquely to the reference genome. Subsequent SNP calling identified 4233 high confidence EMS-induced SNPs between the two

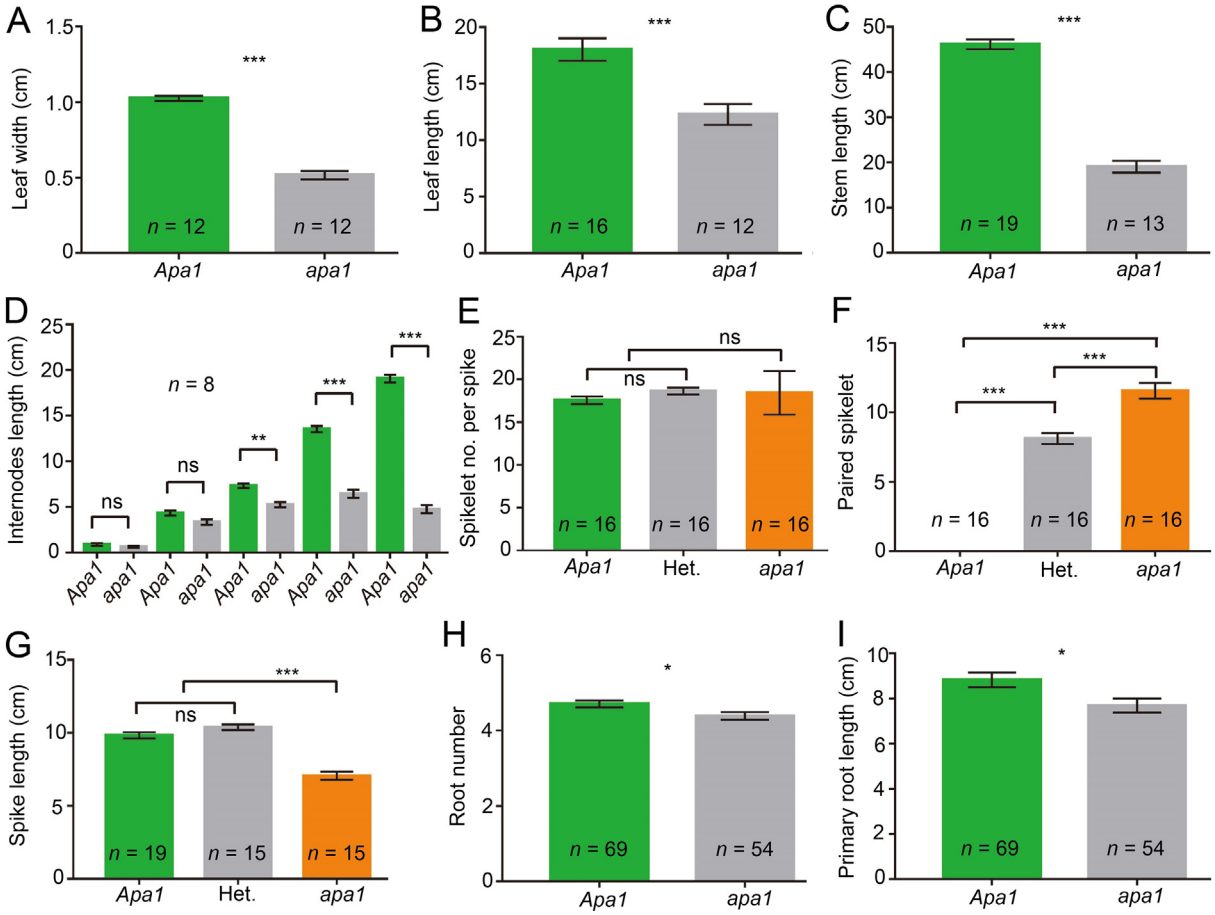

Fig. 2. Effect of the *apa1* mutation on leaf, spike, root, and stem development in wheat. (A) Leaf width; (B) Leaf length; (C) Stem length; (D) Internode lengths; (E) Spikelet number per spike (primary spikelet); (F) Number of paired spikelets (secondary spikelets); (G) Spike length; (H) Root number; and (I) Primary root length. Bars are averages and error bars are standard errors of the mean (SEM). Numbers (*n*) inside the bars indicate the number of plants examined. The asterisks indicate the statistical significance of differences (Dunnett test; ns, not significant; *, $P < 0.05$; **, $P < 0.01$; and ***, $P < 0.001$). *Apa1*, BC_2F_3 plants homozygous for the WT allele; *apa1*, BC_2F_3 plants homozygous for the mutant allele; Het., heterozygous BC_2F_3 plants.

parents. Based on SNP index analysis, we detected 58 SNPs that were significantly associated with the phenotype. Of these 58 significant SNPs, 22 (37.9%) were located on chromosome 1D (Fig. 3) and were mainly distributed in a region from 234.7 to 324.4 Mb (CS RefSeq v1.1, Table S2) suggesting that the *APA1* locus was likely located on chromosome 1D.

3.4. Isolation of the causal gene

To confirm the mapping location, we selected six SNPs (C234740074T, C238067979T, C240594830T, C259211449T, C299584512T, and C365718293T) surrounding the region of interest on chromosome 1D, and developed six D-genome specific CAPS or KASP markers based on these SNPs (Table S1). Using these markers, we genotyped the 168 F_2 plants that had been previously phenotyped and mapped the causal gene to a locus 0.6 cM proximal to the CAPS marker loci *JY2374*, *JY2380*, and *JY2431* (Figs. 4A, B, S4). To define better the position of *APA1*, we then developed two new molecular markers using two SNPs (G201643118A and G217637192A) located proximal to marker locus *JY2374* (C234740074T) and added them to the genetic map (Fig. 4B). Based on this population, *APA1* was tightly linked to marker locus *HB-FR2*, and it mapped to a 1.2 cM region between the marker loci *2018FAB* and *JY2374* (Fig. 4B).

To delimit the position of the *APA1* locus more precisely, we screened another 500 BC_2F_2 plants using the flanking markers *2018FAB* and *JY2374*. We identified 12 plants with informative recombination events in these 500 plants and obtained four recombinants between the same flanking markers used in the previous 168 plants. Using these critical recombinants and three new markers developed in this candidate region, *APA1* was fine mapped to a 0.14 cM interval flanked by marker loci *KP2121* and *KP2150* (Figs. 4C, S4). The 0.14 cM candidate region defines a 3.0 Mb region (215.7–218.7 Mb) in the CS RefSeq v1.1 genome that contains only 11 annotated high-confidence genes (Table S3). Based on BLASTN searches in the wheat expVIP database (https://www.wheat-expression.com/), we found that nine candidate genes were expressed in various wheat tissues (Table S3). These expressed genes included one gene, *TraesCS1D02G155200*, which was annotated as encoding a class III HOMEOBOX LEUCINE-ZIPPER (HD-ZIP III) protein, which is of particular interest because HD-ZIP-type proteins have been reported to be involved in the regulation of leaf, spike, and stem development in the other plants [3,11,12].

Within the candidate chromosomal region, there are only two mutations (G216792764A and G217637192A) between the EMS induced M133 and the parental NC4 line based on RNA sequencing data. Both SNPs co-segregated with the mutant phenotypes (Table S1). The first SNP, G216792764A, is unlikely to be the causal

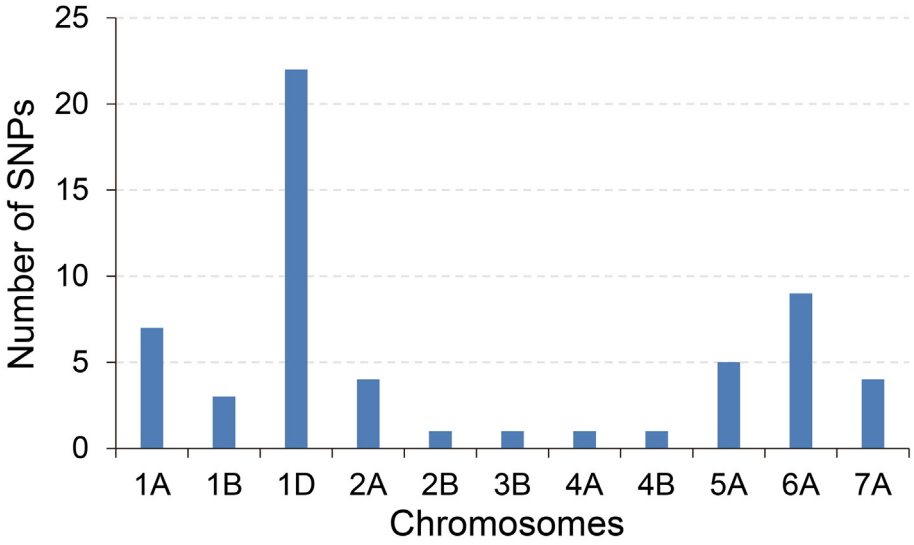

Fig. 3. Distribution of candidate SNPs associated with the mutant phenotype. A total of 22 significant SNPs were located on chromosome 1D.

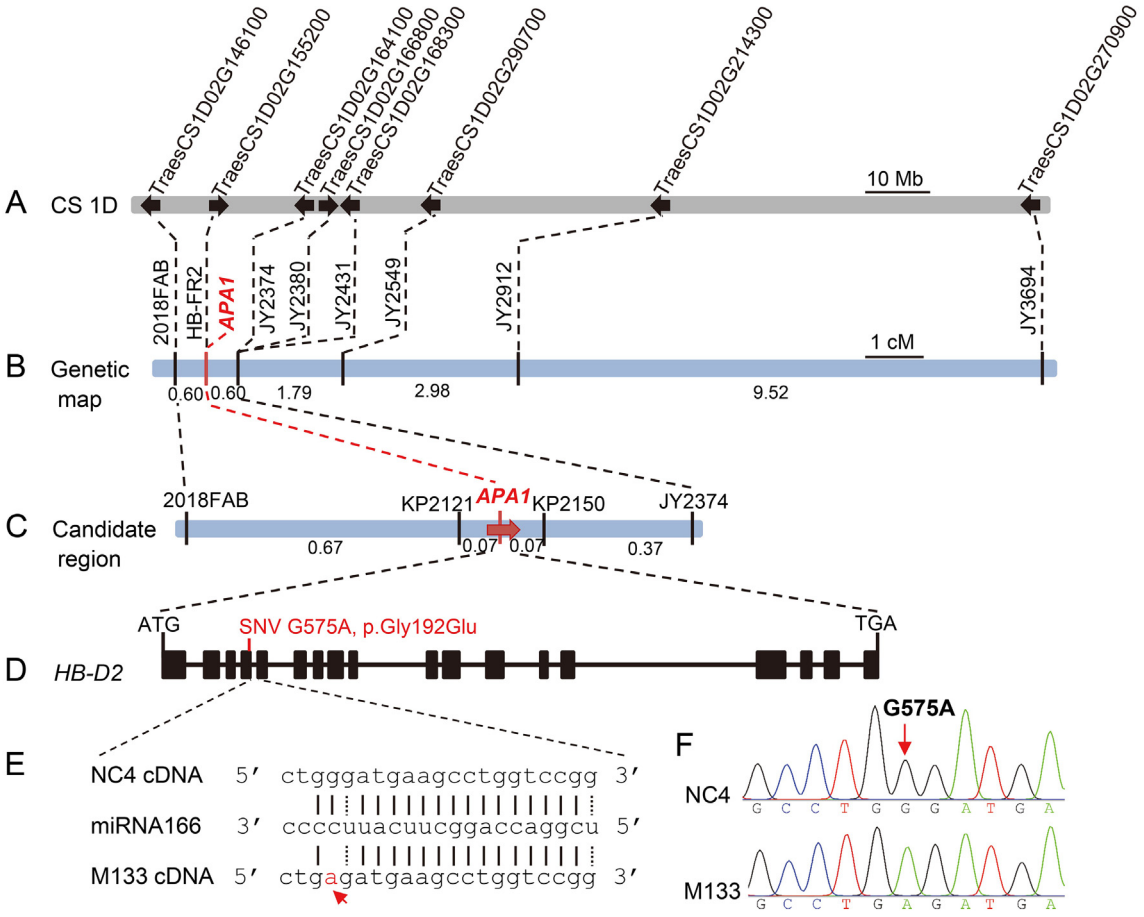

Fig. 4. Map-based cloning of the causal gene. (A) Colinear region on chromosome 1D from the 'Chinese Spring' reference genome (RefSeq v1.1). Arrows indicate genes. (B) Genetic mapping of *APA1* using 336 segregating gametes. (C) High-density map of *APA1* using 1336 segregating gametes and prediction of the candidate gene. (D) Gene structure of the candidate gene *TraesCS1D02G155200* (*HB-D2*). Black rectangles and lines represent exons and introns, respectively; the mutated site in the mutant line M133 is shown in red. (E) Alignment of miRNA166 with the target sites (cDNA coordinates) in NC4 and M133. (F) Sequencing chromatograms showing the G575A polymorphism between the NC4 and M133 alleles. The mutated nucleotide is indicated by a red arrow.

mutation because it is located within an uncharacterized gene that was not annotated in the CS reference genome, while the second SNP, G217637192A, is located within the candidate gene *TraesCS1D02G155200*. Using the primer pair *HB-FR2* (Table S1), we performed PCR to amplify the region including the mutation and confirmed the presence of a single nucleotide transition from G to A (G575A, cDNA coordinates) in the mutant line M133, which results in an amino acid change from glycine to glutamic acid at position 192 from the starting methionine (G192E; BLOSUM62 score = −2; Fig. 4D, F). Further analysis revealed that the mutated site is located in a putative miRNA165/166 target sequence (Fig. 4E), which agrees with the partially dominant nature of the mutation. This semi-dominant resistant allele will be designated hereafter as *rHb-D2*. These results indicate that *TraesCS1D02G155200* is the best candidate for the causal gene among the genes present within the candidate gene region.

3.5. TraesCS1D02G155200 gene structure, phylogenetic analysis, and expression pattern

In NC4, the candidate gene *TraesCS1D02G155200* spans 8,463 bp from the start to the stop codon with a complete coding sequence of 2517 bp (Fig. 4D). This gene is composed of 18 exons interrupted by 17 introns, and it encodes a predicted protein of 838 amino acids. A Neighbor-Joining phylogenetic analysis was carried out to determine the evolutionary relationships between TraesCS1D02G155200 and 42 other HD-Zip III proteins from wheat and six other plant species (Fig. S5). Based on the phylogenetic analysis, the TraesCS1D02G155200 protein was grouped in a clade with OsHB2 from *Oryza sativa* with a high degree (92.6%) of sequence identity (Fig. S5). *TraesCS1D02G155200* is an orthologue of the rice gene *OsHB2* and a paralog of *lateral florets 1* (*lf1*) and *rolled leaf1* (*rld1*) in maize [3,4], and is designated here as *HB2* (*HB-D2*). The A- (*HB-A2*) and B-genome (*HB-B2*) homoeologs are very similar to *HB-D2* with 98.9% and 99.1% sequence identity, respectively.

In general, miRNAs guide the cleavage of target mRNAs by binding to complementary sites [39]. Mutations that disrupt the miRNA complementary sites are known to influence miRNA-mediated cleavage *in vivo* [3,4,40,41]. We analyzed *HB-D2* transcript levels relative to *ACTIN* in BC_2F_3 plants homozygous for the WT and mutant alleles by qPCR. The expression data for *HB-D2* in leaves, roots, stems, and spikes showed that its transcripts accumulated in all tissues at significantly higher levels in the plants carrying the resistant *rHb-D2* allele compared to the *Hb-D2* WT allele ($P < 0.01$; Fig. 5). This result suggests that, due to the disruption of the miRNA165/166 complementary site, the mRNA from the resistant *rHb-D2* allele is not degraded by miRNA165/166 as efficiently as the WT allele. Transcript levels of *HB-A2* and *HB-B2* were also evaluated using two genome-specific qRT-PCR primers (Table S1), and they showed similar levels to *HB-D2* in the BC_2F_3 plants carrying the WT alleles (Fig. S6). Finally, analysis of RNA-seq data available in the wheat expVIP database (https://www.wheat-expression.com/) showed similar expression profiles (Fig. S7). Transcripts of *HB-D2*, *HB-A2*, and *HB-B2* were detected in different organs and tissues.

3.6. The rHb-A2 and rHb-B2 EMS mutants show phenotypic alterations

A search of the sequenced EMS-mutagenized populations derived from wheat cultivars 'Cadenza' and 'Jimai 22' yielded two mutants for *HB-D2*. Mutant lines Cadenza1290 and jm_chr1D_217637192 carry the same mutation G217637192A as in M133 (Fig. S8). However, seeds of both mutant lines were not available likely due to the reduced fertility of the mutants.

We then searched for mutations in the miR165/166 binding site of *HB-A2* and *HB-B2*. We obtained one 'Cadenza' mutant line, Cadenza1761, for *HB-A2*, which carries the mutation G580A (G194R; BLOSUM62 score =−2) located in the miRNA165/166 complementary site (Figs. 6A, S9). For the B-genome homoeolog *HB-B2*, we identified the 'Cadenza' mutant line Cadenza0269 that has a single nucleotide change C589T (P197S; BLOSUM62 score =−1) in the miRNA166 complementary site (Figs. 6B, S9). Using the genome-specific primer pairs *CaA1761* and *CaB0269* (Table S1), we genotyped 20 plants from each of the selected mutant lines. We identified six plants that were homozygous for the *rHb-A2* allele, nine plants homozygous for the WT allele, and five heterozygous plants in the line Cadenza1761. In the mutant line Cadenza0269, we detected four homozygous mutant plants, 14 homozygous WT plants, and two heterozygous plants. In a greenhouse experiment, we observed that the plants homozygous for the *rHb-A2* mutant allele exhibited paired spikelets and reduced plant height (Fig. 6A). But we could not determine whether these homozygous *rHb-A2* plants formed upward-curled leaves since the plants homozygous for the WT allele in this mutant line also showed some degree of leaf curling (Fig. 6A).

For the plants carrying the *rHb-B2* allele, we also observed similar mutant phenotypes (Fig. 6B), but the intensity of these phenotypic defects was lower than in the *rHb-A2* homozygous mutant plants (Fig. 6). As shown in Fig. 6B, some of the secondary spikelets developed into needle-like structures in the *rHb-B2* mutant. The smaller phenotypic effects of the *rHb-B2* mutation relative to *rHb-A2* may be related to the smaller disruptive effect of the predicted amino acid changes, since the predicted minimum free energy (mfe) of the interactions between miRNA and the target sites were very similar (Fig. S10). The larger difference in mfe in M133 may have contributed to its stronger phenotype (Fig. S10).

3.7. rHb-D2 transgenic plants exhibit obvious abnormalities

Previous studies have reported that overexpression of the mutated resistant versions of *HD-Zip III* genes resulted in abnormalities such as rolled leaves and lateral florets from ectopic expression of these genes in corresponding tissues [3,5,13,42]. To determine whether *rHb-D2* has the same effects, we generated 12 independent T_0 transgenic plants expressing *rHb-D2* driven by the maize UBI promoter. The presence of the *rHb-D2* transgene in these plants was confirmed using the primer pair *HB-JCX* (Table S1). Transcript levels of *rHb-D2* were significantly higher ($P < 0.001$) in all transgenic plants than in the non-transgenic 'Fielder' control plants (Fig. S11). Transgenic plants grown in a growth chamber environment (25 °C day/23 °C night and 18 h light/6 h dark photoperiod) displayed severe leaf rolling and extreme dwarfism (Fig. 7A, B). At maturity, some of the transgenic plants (e.g. mT_0-09 and mT_0-12) showed paired spikelets (Fig. 7C). In addition, plants from T_1 transgenic families mT_1-09 and mT_1-12 carrying the transgene showed the rolled-leaf phenotype (Fig. 7D).

The extreme phenotype of the transgenic plants is likely the result of a combination between the high expression levels generated by the UBI promoter and the reduced mRNA degradation generated by the mutation in the miRNA165/166 binding site in the constitutively expressed the resistant *rHb-D2* allele. Taken together, the high-resolution genetic map, the independent mutants, and the transgenic plants confirm that *TraesCS1D02G155200* (*HB-D2*) is the causal gene for the abnormal plant architecture associated with *APA1* locus in the M133 mutant.

3.8. Natural variation in HB2

In order to determine the allelic variations in *HB-D2*, *HB-A2*, and *HB-B2*, a total of 15 published reference genomes and 1382 wheat

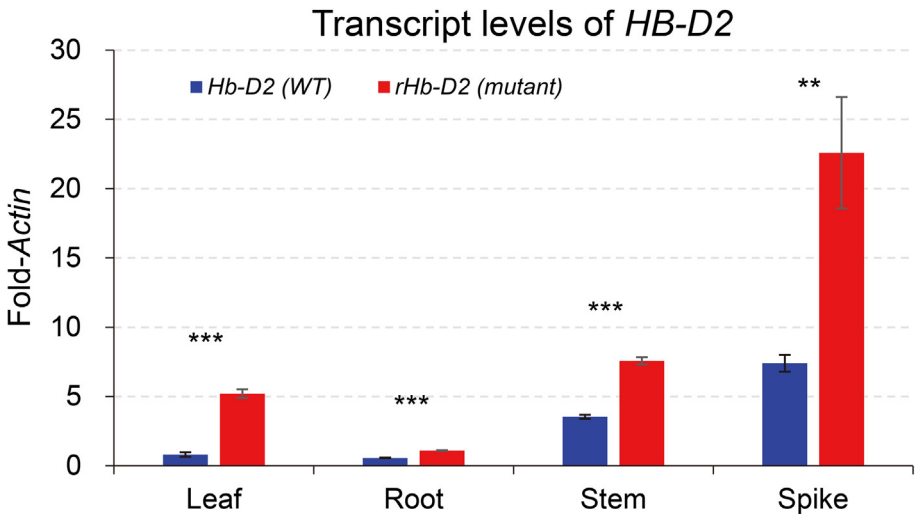

Fig. 5. *HB-D2* mRNA levels in BC_2F_3 sister plants homozygous for either the WT or mutant alleles. Plants were grown in growth chambers at 25 °C day/23 °C night with an 18 h light/6 h dark photoperiod. Leaves and roots were collected at the two-leaf stage, stems at the heading stage, and young spikes were collected when they were ~10 mm in length. Transcript levels were normalized relative to *ACTIN* gene that was used as endogenous control (n = 4). Error bars indicate the SEM. The asterisks indicate the statistical significance of the differences (ns, not significant; *, $P < 0.05$; **, $P < 0.01$; and ***, $P < 0.001$). *Hb-D2*, BC_2F_3 plants homozygous for the WT allele; *rHb-D2*, BC_2F_3 plants homozygous for the mutant allele.

genotypes with exome sequencing data derived from the 500 exomes project [37], the 1000 wheat exomes project (includes 811 wheat genotypes after imputation and filtering) [36], and the 59 exomes project (generated in WheatCAP project) [38], were used for comparative analysis. Our survey found that HB-D2 is highly conserved among different wheat genotypes with only four rare amino acid polymorphisms (Table S4). For HB-A2 and HB-B2, we detected 12 and 8 amino acid polymorphisms, respectively (Table S4). However, no SNPs were observed in the complementary sites for miRNA165/166 in the three *HB2* homoeologs among these 1397 wheat accessions, indicating that these sequences are highly conserved.

4. Discussion

4.1. Identification of HB-D2 as the causal gene of the morphological changes in the M133 mutant

Leaf, spike, stem, and root morphologies are complex traits controlled by multiple genes. In rice and other plant species, many genes/QTL associated with these morphological traits have been mapped or cloned [4,7,43,44]. Genetic intervals controlling leaf, spike, stem, and root morphological changes have been also reported in wheat, but it was previously difficult to isolate the causal genes due to the large and complex nature of the wheat genome [45–47]. Fortunately, the recently released wheat genomes and the availability of new high throughput sequencing tools have made this task feasible.

BSR-seq, a recently-developed method that combines BSA with RNA-seq, has been used to identify major genes in a number of different plant species, including maize [48], wheat [49], cabbage [50], and soybean [51]. Using BSR-seq analysis and the publicly available wheat genome sequences, we were able to rapidly map the causal gene region, which included *HB-D2* (*TraesCS1D02G155200*). This gene encodes a class III homeodomain-leucine zipper (HD-ZIP III) transcription factor, a gene family that has been associated with morphological changes in other plant species [3,4,11,12].

4.2. Effect of miRNA165/166 resistant alleles in different plant species

The mutations in many gain-of-function mutants of *HD-ZIP III* genes, such as *rev*, *phb*, and *phv* in Arabidopsis, *rld1* in maize, and *lf1* in rice, were all found to be located within the miRNA165/166 complementary site [3,4,52]. In this study, we detected a single nucleotide substitution (G575A, Fig. 4) in *HB-D2* that disrupted the base pairing at the 3′ end of miRNA165/166. This mutation caused multiple phenotypic changes, the most serious of which included upward-curling leaves, paired spikelets, and dwarfism (Fig. 1). The same nucleotide substitution was reported in the miRNA165/166 complementary site of *rld1* in the maize *Rld1-O* mutant [4].

The phylogenetic analysis of the HD-ZIP III proteins from seven plant species showed that HB-D2, RLD1, and LF1 cluster together in the same clade (Fig. S5). In maize, gain-of-function mutations in *Rld1* were mainly involved in leaf polarity regulation [4]. In rice, a single mutation within the miRNA165/166 binding site of the *lf1* gene caused curled leaves and three-floret spikelets [3,5]. We noticed that the upward curling of the leaves in the *rHb-D2* mutant is similar to the leaf development defects in *Rld1-O* and *lf1* mutant plants, indicating a conserved function for these *HD-ZIP III* genes in rice, maize, and wheat. However, in addition to the rolled-leaf phenotype, we also observed other morphological changes in *rHb-D2* mutant plants that were not observed in the *Rld1-O* and *lf1* mutants, suggesting that these genes may have some degree of functional differentiation in the different plant species. However, phenotypes such as the paired spikelets may be associated with the different architecture of the wheat inflorescence.

Gain-of-function phenotypes due to *HD-ZIP III* genes caused by mutations in the miRNA binding sites and increased expression are easier to detect than recessive mutations. In Arabidopsis, ectopic expression of the *HD-ZIP III* genes *PHB*, *REV*, and *PHV* results in the formation of radially symmetrical leaves [40,41,53]. Ectopic expression of *LF1* in rice causes lateral florets to develop at the axil of the sterile lemma [3]. The changes observed in these species are similar to those observed here in wheat, suggesting that the disruption of the miRNA binding site and the resulting increased expression is a common mechanism underlying these phenotypes [3,54]. This hypothesis is supported by the similar genotypes gen-

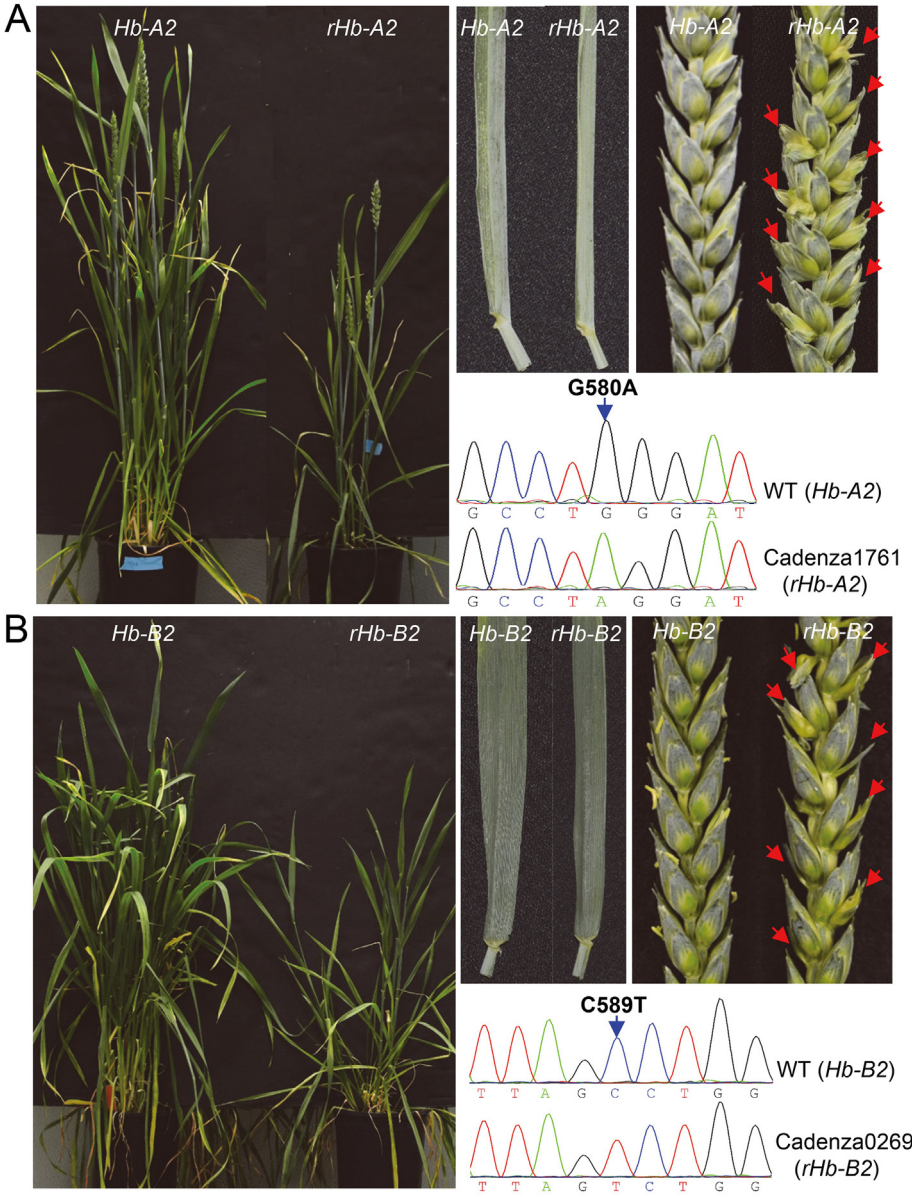

Fig. 6. *rHb-A2* and *rHb-B2* EMS mutant plants showing phenotypic changes relative to plants homozygous for the WT allele. (A) Visual phenotypes of plants homozygous for the WT (*Hb-A2*) and mutant (*rHb-A2*) alleles in the line Cadenza1761 and sequencing chromatograms showing the G580A polymorphism. (B) Visual phenotypes of plants homozygous for the WT (*Hb-B2*) and mutant (*rHb-B2*) alleles in the line Cadenza0269 and sequencing chromatograms showing the C589T polymorphism. The mutated nucleotides are indicated by blue arrows. Paired spikelets are indicated by red arrows.

erated in this study by the overexpression of the miRNA-resistant allele of *HB-D2* in wheat (Fig. 7). In rice, overexpression of miR166-resistant versions of *HD-ZIP III* genes resulted in morphological changes whereas over-expression of the WT versions did not [3,13].

4.3. Effect of different mutations and environmental conditions on HB2

We observed plants carrying *rHb-D2*, *rHb-A2*, and *rHb-B2* mutant plants displayed varying degrees of phenotypic effects (Figs. 4, 6). The *rHb-D2* mutant showed the strongest phenotypic effect followed closely by *rHb-A2*, whereas *rHb-B2* displayed the weakest effect. This gradient of phenotypic effects may be the result of the combination of two different effects: the stronger disruptive effect of *rHb-D2* and *rHb-A2* on the predicted amino acid changes (smaller BLOSUM62 values) and the larger effect of *rHb-D2* on the predicted minimum free energy of the interaction with the miRNA relative to the other two mutations (Fig. S10). The different locations of the mutations may also contribute to the different intensity of the phenotypes. Similarly to the *Rld1-O* mutant in maize [4], the *rHb-D2* and *rHb-A2* mutations disrupt pairing at the 3′ end of miRNA165/166 (Figs. 4, S9), whereas *rHb-B2* affects a more central part of the miRNA binding site (Fig. S9).

Several *HD-ZIP* genes are known to be associated with changes in heading date or flowering time, such as *sgd2* [55] and *Roc4* [56]. Our data demonstrate that the *rHb-D2* mutation was also associated with 8.8 days delay in heading time when the plants were grown in a growth chamber at 10 °C with a 12 h photoperiod (Fig. S3). However, the effect on heading time was reduced when the plants were grown under a longer photoperiod and at higher temperature. By contrast, the intensity of some morphological defects (e.g., rolled leaf and dwarfism) observed in the plants carrying the resistant *rHb-D2* allele were milder when plants were grown at 10 °C/12 h photoperiod than when they were grown at

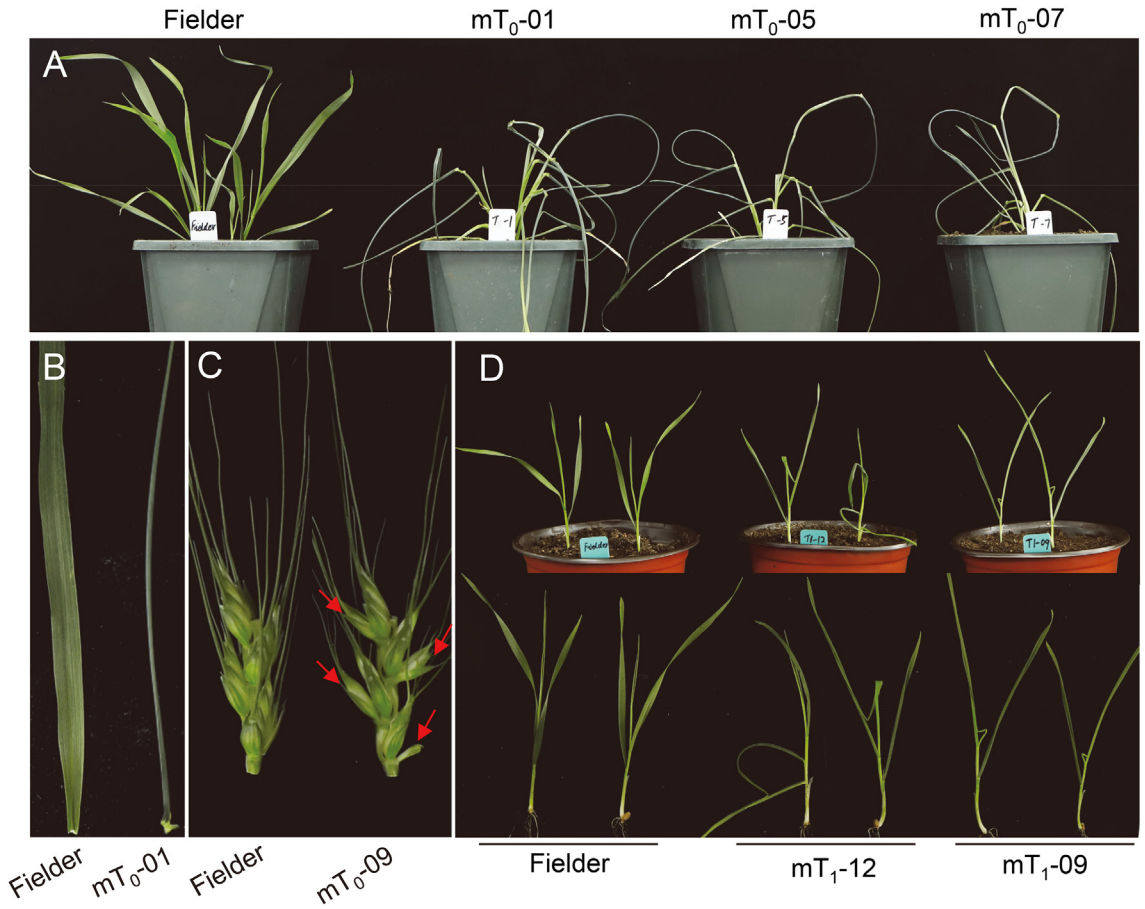

Fig. 7. Phenotypic effects of *rHb-D2* overexpression in transgenic plants of the wheat cultivar 'Fielder'. (A) Phenotypes of the T_0 transgenic plants mT_0-01, mT_0-05, and T_0-07 overexpressing *rHb-D2* compared to the non-transgenic 'Fielder' control. (B) Representative images of leaves from the mT_0-01 transgenic and control plants. (C) Representative images of spikes from the mT_0-09 transgenic and control plants. Red arrows indicate the paired spikelets. (D) Phenotypes of the T_1 transgenic families mT_1-09 and mT_1-12 overexpressing *rHb-D2* compared to the non-transgenic 'Fielder' control.

higher temperatures and longer photoperiods (Fig. S3). These results suggest that photoperiod or/and temperature may modulate some of the effects of miRNA165/166 or its target genes, a result not reported in previous studies.

Although the changes in heading time and the increases in the number of secondary spikelets (paired spikelets) could be beneficial for wheat improvement, the multiple pleiotropic effects of the miRNA165/166 resistant *rHb2* alleles preclude their direct use in agriculture. The study of the targets of this transcription factor may help to dissect these different effects, and separate beneficial and detrimental effects. The validation of *HB-D2* as the causal gene affecting the development of leaves, spikes, roots, and stems is a first step in that direction and contributes to a better understanding of the regulation of morphological traits in wheat.

CRediT authorship contribution statement

Dengji Jiang: Data curation, Investigation, Formal analysis, Visualization, Validation, Writing – original draft. **Lei Hua:** Data curation, Investigation, Formal analysis, Visualization, Validation, Writing – original draft. **Chaozhong Zhang:** Data curation, Investigation, Formal analysis, Visualization, Validation, Writing – original draft. **Hongna Li:** Software, Formal analysis, Visualization. **Zheng Wang:** Resources. **Jian Li:** Resources. **Guiping Wang:** Software, Formal analysis, Visualization, Resources. **Rui Song:** Software, Formal analysis, Visualization. **Tao Shen:** Software, Formal analysis, Visualization. **Hongyu Li:** Software, Formal analysis, Visualization. **Shengsheng Bai:** Software, Formal analysis, Visualization. **Yanna Liu:** Software, Formal analysis, Visualization. **Jian Wang:** Software, Formal analysis, Visualization. **Hao Li:** Resources. **Jorge Dubcovsky:** Resources, Funding acquisition, Writing – review & editing. **Shisheng Chen:** Project administration, Methodology, Funding acquisition, Writing – original draft, Writing – review & editing.

Data availability

Raw sequencing data generated in this project has been deposited in NCBI's Sequence Read Archive (https://www.ncbi.nlm.nih.gov/sra, Bioproject PRJNA826248).

Declaration of competing interest

The authors declare that they have no known competing financial interests or personal relationships that could have appeared to influence the work reported in this paper.

Acknowledgments

We thank Juan Debernardi (UCD) for his suggestions on the analyses of the miRNA data. Work at SC lab was supported by the Provincial Natural Science Foundation of Shandong (ZR2021MC056 and ZR2021ZD30) and the Open Project Funding of the State Key Laboratory of Crop Stress Adaptation and Improve-

ment. Research at JD lab was funded by Competitive Grant 2022-68013-36439 (WheatCAP) from the USDA National Institute of Food and Agriculture.

Appendix A. Supplementary data

Supplementary data for this article can be found online at https://doi.org/10.1016/j.cj.2022.05.002.

References

[1] S.A. Harrington, N. Cobo, M. Karafiátová, J. Doležel, P. Borrill, C. Uauy, Identification of a dominant chlorosis phenotype through a forward screen of the *Triticum turgidum* cv. Kronos TILLING population, Front. Plant Sci. 10 (2019) 963.

[2] P.B. Talbert, H.T. Adler, D.W. Parks, L. Comai, The *REVOLUTA* gene is necessary for apical meristem development and for limiting cell divisions in the leaves and stems of *Arabidopsis thaliana*, Development 121 (1995) 2723–2735.

[3] T. Zhang, Y. Li, L. Ma, X. Sang, Y. Ling, Y. Wang, P. Yu, H. Zhuang, J. Huang, N. Wang, F. Zhao, C. Zhang, Z. Yang, L. Fang, G. He, *LATERAL FLORET 1* induced the three-florets spikelet in rice, Proc. Natl. Acad. Sci. U. S. A. 114 (2017) 9984–9989.

[4] M.T. Juarez, J.S. Kui, J. Thomas, B.A. Heller, M.C.P. Timmermans, microRNA-mediated repression of *rolled leaf1* specifies maize leaf polarity, Nature 428 (2004) 84–88.

[5] T. Zhang, J. You, Y.i. Zhang, W. Yao, W. Chen, Q. Duan, W. Xiao, L.i. Ye, Y. Zhou, X. Sang, Y. Ling, G. He, Y. Li, *LF1* regulates the lateral organs polarity development in rice, New Phytol. 231 (2021) 1265–1277.

[6] M. Li, G. Xiong, R. Li, J. Cui, D. Tang, B. Zhang, M. Pauly, Z. Cheng, Y. Zhou, Rice cellulose synthase-like D4 is essential for normal cell-wall biosynthesis and plant growth, Plant J. 60 (2009) 1055–1069.

[7] J. Hu, L.i. Zhu, D. Zeng, Z. Gao, L. Guo, Y. Fang, G. Zhang, G. Dong, M. Yan, J. Liu, Q. Qian, Identification and characterization of *NARROW AND ROLLED LEAF 1*, a novel gene regulating leaf morphology and plant architecture in rice, Plant Mol. Biol. 73 (2010) 283–292.

[8] W. Luan, Y. Liu, F. Zhang, Y. Song, Z. Wang, Y. Peng, Z. Sun, *OsCD1* encodes a putative member of the cellulose synthase-like D sub-family and is essential for rice plant architecture and growth, Plant Biotechnol. J. 9 (2011) 513–524.

[9] S.P. Grigg, C. Galinha, N. Kornet, C. Canales, B. Scheres, M. Tsiantis, Repression of apical homeobox genes is required for embryonic root development in *Arabidopsis*, Curr. Biol. 19 (2009) 1485–1490.

[10] A. Carlsbecker, J.Y. Lee, C.J. Roberts, J. Dettmer, S. Lehesranta, J. Zhou, O. Lindgren, M.A. Moreno-Risueno, A. Vatén, S. Thitamadee, A. Campilho, J. Sebastian, J.L. Bowman, Y. Helariutta, P.N. Benfey, Cell signalling by microRNA165/6 directs gene dose-dependent root cell fate, Nature 465 (2010) 316–321.

[11] M.J. Prigge, D. Otsuga, J.M. Alonso, J.R. Ecker, G.N. Drews, S.E. Clark, Class III *homeodomain-leucine zipper* gene family members have overlapping, antagonistic, and distinct roles in *Arabidopsis* development, Plant Cell 17 (2005) 61–76.

[12] G. Hu, J. Fan, Z. Xian, W. Huang, D. Lin, Z. Li, Overexpression of *SlREV* alters the development of the flower pedicel abscission zone and fruit formation in tomato, Plant Sci. 229 (2014) 86–95.

[13] J.I. Itoh, K.I. Hibara, Y. Sato, Y. Nagato, Developmental role and auxin responsiveness of Class III homeodomain leucine zipper gene family members in rice, Plant Physiol. 147 (2008) 1960–1975.

[14] F.D. Ariel, P.A. Manavella, C.A. Dezar, R.L. Chan, The true story of the HD-Zip family, Trends Plant Sci. 12 (2007) 419–426.

[15] A. Agalou, S. Purwantomo, E. Övernäs, H. Johannesson, X. Zhu, A. Estiati, R.J. de Kam, P. Engström, I.H. Slamet-Loedin, Z. Zhu, M. Wang, L. Xiong, A.H. Meijer, P. B.F. Ouwerkerk, A genome-wide survey of HD-Zip genes in rice and analysis of drought-responsive family members, Plant Mol. Biol. 66 (2008) 87–103.

[16] Z. Wang, J. Li, S. Chen, Y. Heng, Z. Chen, J. Yang, K. Zhou, J. Pei, H. He, X.W. Deng, L. Ma, Poaceae-specific *MS1* encodes a phospholipid-binding protein for male fertility in bread wheat, Proc. Natl. Acad. Sci. U. S. A. 114 (2017) 12614–12619.

[17] A.M. Bolger, M. Lohse, B. Usadel, Trimmomatic: a flexible trimmer for Illumina sequence data, Bioinformatics 30 (2014) 2114–2120.

[18] The International Wheat Genome Sequencing Consortium, Shifting the limits in wheat research and breeding using a fully annotated reference genome, Science 361 (2018) eaar7191.

[19] A. Dobin, C.A. Davis, F. Schlesinger, J. Drenkow, C. Zaleski, S. Jha, P. Batut, M. Chaisson, T.R. Gingeras, STAR: ultrafast universal RNA-seq aligner, Bioinformatics 29 (2013) 15–21.

[20] A. McKenna, M. Hanna, E. Banks, A. Sivachenko, K. Cibulskis, A. Kernytsky, K. Garimella, D. Altshuler, S. Gabriel, M. Daly, M.A. DePristo, The Genome Analysis Toolkit: a MapReduce framework for analyzing next-generation DNA sequencing data, Genome Res. 20 (2010) 1297–1303.

[21] H. Takagi, A. Abe, K. Yoshida, S. Kosugi, S. Natsume, C. Mitsuoka, A. Uemura, H. Utsushi, M. Tamiru, S. Takuno, H. Innan, L.M. Cano, S. Kamoun, R. Terauchi, QTL-seq: rapid mapping of quantitative trait loci in rice by whole genome resequencing of DNA from two bulked populations, Plant J. 74 (2013) 174–183.

[22] A. Abe, S. Kosugi, K. Yoshida, S. Natsume, H. Takagi, H. Kanzaki, H. Matsumura, K. Yoshida, C. Mitsuoka, M. Tamiru, H. Innan, L. Cano, S. Kamoun, R. Terauchi, Genome sequencing reveals agronomically important loci in rice using MutMap, Nat. Biotechnol. 30 (2012) 174–178.

[23] A. Konieczny, F.M. Ausubel, A procedure for mapping *Arabidopsis* mutations using co-dominant ecotype-specific PCR-based markers, Plant J. 4 (1993) 403–410.

[24] LGC Genomics, KASP™ Genotyping Chemistry User Guide and Manual, http://www.lgcgenomics.com/genotyping/kasp-genotyping-reagents/?download_file=22_1_kasp_manual.pdf&download_cat=downloads, 2013.

[25] S. Kumar, G. Stecher, K. Tamura, MEGA7: molecular evolutionary genetics analysis version 7.0 for bigger datasets, Mol. Biol. Evol. 33 (2016) 1870–1874.

[26] W. Zhang, S. Chen, Z. Abate, J. Nirmala, M.N. Rouse, J. Dubcovsky, Identification and characterization of *Sr13*, a tetraploid wheat gene that confers resistance to the Ug99 stem rust race group, Proc. Natl. Acad. Sci. U. S. A. 114 (2017) E9483–E9492.

[27] S. Pearce, L.S. Vanzetti, J. Dubcovsky, Exogenous gibberellins induce wheat spike development under short days only in the presence of *VERNALIZATION 1*, Plant Physiol. 163 (2013) 1433–1445.

[28] K.V. Krasileva, H. Vasquez-Gross, T. Howell, P. Bailey, F. Paraiso, L. Clissold, J. Simmonds, R.H. Ramirez-Gonzalez, X. Wang, P. Borrill, C. Fosker, S. Ayling, A. Phillips, C. Uauy, J. Dubcovsky, Uncovering hidden variation in polyploid wheat, Proc. Natl. Acad. Sci. U. S. A. 114 (2017) E913–E921.

[29] M. Rehmsmeier, P. Steffen, M. Höchsmann, R. Giegerich, Fast and effective prediction of microRNA/target duplexes, RNA 10 (2004) 1507–1517.

[30] H. Ling, B. Ma, X. Shi, H. Liu, Li. Dong, H. Sun, Y. Cao, Q. Gao, S. Zheng, Y. Li, Y. Yu, H. Du, M. Qi, Y. Li, H. Lu, H. Yu, Y. Cui, N. Wang, C. Chen, H. Wu, Y. Zhao, J. Zhang, Y. Li, W. Zhou, B. Zhang, W. Hu, M.J.T. van Eijk, J. Tang, H.M.A. Witsenboer, S. Zhao, Z. Li, A. Zhang, D. Wang, C. Liang, Genome sequence of the progenitor of wheat A subgenome *Triticum urartu*, Nature 557 (2018) 424–428.

[31] M. Luo, Y. Gu, D. Puiu, H. Wang, S.O. Twardziok, K.R. Deal, N. Huo, T. Zhu, L. Wang, Y. Wang, P.E. McGuire, S. Liu, H. Long, R.K. Ramasamy, J.C. Rodriguez, S. L. Van, L. Yuan, Z. Wang, Z. Xia, L. Xiao, O.D. Anderson, S. Ouyang, Y. Liang, A.V. Zimin, G. Pertea, P. Qi, J.L. Bennetzen, X. Dai, M.W. Dawson, H.G. Müller, K. Kugler, L. Rivarola-Duarte, M. Spannagl, K.F.X. Mayer, F. Lu, M.W. Bevan, P. Leroy, P. Li, F.M. You, Q. Sun, Z. Liu, E. Lyons, T. Wicker, S.L. Salzberg, K.M. Devos, J. Dvořák, Genome sequence of the progenitor of the wheat D genome *Aegilops tauschii*, Nature 551 (2017) 498–502.

[32] M. Maccaferri, N.S. Harris, S.O. Twardziok, R.K. Pasam, H. Gundlach, M. Spannagl, D. Ormanbekova, T. Lux, V.M. Prade, S.G. Milner, A. Himmelbach, M. Mascher, P. Bagnaresi, P. Faccioli, P. Cozzi, M. Lauria, B. Lazzari, A. Stella, A. Manconi, M. Gnocchi, M. Moscatelli, R. Avni, J. Deek, S. Biyiklioglu, E. Frascaroli, S. Corneti, S. Salvi, G. Sonnante, F. Desiderio, C. Marè, C. Crosatti, E. Mica, H. Özkan, B. Kilian, P. De Vita, D. Marone, R. Joukhadar, E. Mazzucotelli, D. Nigro, A. Gadaleta, S. Chao, J.D. Faris, A.T.O. Melo, M. Pumphrey, N. Pecchioni, L. Milanesi, K. Wiebe, J. Ens, R.P. MacLachlan, J.M. Clarke, A.G. Sharpe, C.S. Koh, K. Y.H. Liang, G.J. Taylor, R. Knox, H. Budak, A.M. Mastrangelo, S.S. Xu, N. Stein, L. Hale, A. Distelfeld, M.J. Hayden, R. Tuberosa, S. Walkowiak, K.F.X. Mayer, A. Ceriotti, C.J. Pozniak, L. Cattivelli, Durum wheat genome highlights past domestication signatures and future improvement targets, Nat. Genet. 51 (2019) 885–895.

[33] R. Avni, M. Nave, O. Barad, K. Baruch, S.O. Twardziok, H. Gundlach, L. Hale, M. Mascher, M. Spannagl, K. Wiebe, K.W. Jordan, G. Golan, J. Deek, B. Ben-Zvi, G. Ben-Zvi, A. Himmelbach, R.P. MacLachlan, A.G. Sharpe, A. Fritz, R. Ben-David, H. Budak, T. Fahima, A. Korol, J.D. Faris, A. Hernandez, M.A. Mikel, A.A. Levy, B. Steffenson, M. Maccaferri, R. Tuberosa, L. Cattivelli, P. Faccioli, A. Ceriotti, K. Kashkush, M. Pourkheirandish, T. Komatsuda, T. Eilam, H. Sela, A. Sharon, N. Ohad, D.A. Chamovitz, K.F.X. Mayer, N. Stein, G. Ronen, Z. Peleg, C.J. Pozniak, E. D. Akhunov, A. Distelfeld, Wild emmer genome architecture and diversity elucidate wheat evolution and domestication, Science 357 (2017) 93–97.

[34] S. Walkowiak, L. Gao, C. Monat, G. Haberer, M.T. Kassa, J. Brinton, R.H. Ramirez-Gonzalez, M.C. Kolodziej, E. Delorean, D. Thambugala, V. Klymiuk, B. Byrns, H. Gundlach, V. Bandi, J.N. Siri, K. Nilsen, C. Aquino, A. Himmelbach, D. Copetti, T. Ban, L. Venturini, M. Bevan, B. Clavijo, D. Koo, J. Ens, K. Wiebe, A. N'Diaye, A.K. Fritz, C. Gutwin, A. Fiebig, C. Fosker, B. Fu, G.G. Accinelli, K.A. Gardner, N. Fradgley, J. Gutierrez-Gonzalez, G. Halstead-Nussloch, M. Hatakeyama, C.S. Koh, J. Deek, A.C. Costamagna, P. Fobert, D. Heavens, H. Kanamori, K. Kawaura, F. Kobayashi, K. Krasileva, T. Kuo, N. McKenzie, K. Murata, Y. Nabeka, T. Paape, S. Padmarasu, L. Percival-Alwyn, S. Kagale, U. Scholz, J. Sese, P. Juliana, R. Singh, R. Shimizu-Inatsugi, D. Swarbreck, J. Cockram, H. Budak, T. Tameshige, T. Tanaka, H. Tsuji, J. Wright, J. Wu, B. Steuernagel, I. Small, S. Cloutier, G. Keeble-Gagnère, G. Muehlbauer, J. Tibbets, S. Nasuda, J. Melonek, P.J. Hucl, A.G. Sharpe, M. Clark, E. Legg, A. Bharti, P. Langridge, A. Hall, C. Uauy, M. Mascher, S.G. Krattinger, H. Handa, K.K. Shimizu, A. Distelfeld, K. Chalmers, B. Keller, K.F.X. Mayer, J. Poland, N. Stein, C.A. McCartney, M. Spannagl, T. Wicker, C.J. Pozniak, Multiple wheat genomes reveal global variation in modern breeding, Nature 588 (2020) 277–283.

[35] K. Sato, F. Abe, M. Mascher, G. Haberer, H. Gundlach, M. Spannagl, K. Shirasawa, S. Isobe, Chromosome-scale genome assembly of the transformation-amenable common wheat cultivar 'Fielder', DNA Res 28 (2021) dsab008.

[36] F. He, R. Pasam, F. Shi, S. Kant, G. Keeble-Gagnere, P. Kay, K. Forrest, A. Fritz, P. Hucl, K. Wiebe, R. Knox, R. Cuthbert, C. Pozniak, A. Akhunova, P.L. Morrell, J.P. Davies, S.R. Webb, G. Spangenberg, B. Hayes, H. Daetwyler, J. Tibbits, M. Hayden, E. Akhunov, Exome sequencing highlights the role of wild-relative

introgression in shaping the adaptive landscape of the wheat genome, Nat. Genet. 51 (2019) 896–904.
[37] C. Pont, T. Leroy, M. Seidel, A. Tondelli, W. Duchemin, D. Armisen, D. Lang, D. Bustos-Korts, N. Goué, F. Balfourier, M. Molnár-Láng, J. Lage, B. Kilian, H. Özkan, D. Waite, S. Dyer, T. Letellier, M. Alaux, J. Russell, B. Keller, F. van Eeuwijk, M. Spannagl, K.F.X. Mayer, R. Waugh, N. Stein, L. Cattivelli, G. Haberer, G. Charmet, J. Salse, Tracing the ancestry of modern bread wheats, Nat. Genet. 51 (2019) 905–911.
[38] S. Chen, J. Hegarty, T. Shen, L. Hua, H. Li, J. Luo, H. Li, S. Bai, C. Zhang, J. Dubcovsky, Stripe rust resistance gene *Yr34* (synonym *Yr48*) is located within a distal translocation of *Triticum monococcum* chromosome $5A^{m}L$ into common wheat, Theor. Appl. Genet. 134 (2021) 2197–2211.
[39] M.W. Rhoades, B.J. Reinhart, L.P. Lim, C.B. Burge, B. Bartel, D.P. Bartel, Prediction of plant microRNA targets, Cell 110 (4) (2002) 513–520.
[40] J.R. McConnell, J. Emery, Y. Eshed, N. Bao, J. Bowman, M.K. Barton, Role of *PHABULOSA* and *PHAVOLUTA* in determining radial patterning in shoots, Nature 411 (2001) 709–713.
[41] J.F. Emery, S.K. Floyd, J. Alvarez, Y. Eshed, N.P. Hawker, A. Izhaki, S.F. Baum, J.L. Bowman, Radial patterning of *Arabidopsis* shoots by class III *HD-ZIP* and *KANADI* genes, Curr. Biol. 13 (2003) 1768–1774.
[42] Y. Li, A. Shen, W. Xiong, Q. Sun, Q. Luo, T. Song, Z. Li, W. Luan, Overexpression of *OsHox32* results in pleiotropic effects on plant type architecture and leaf development in rice, Rice 9 (2016) 46–60.
[43] Q. Zhang, T. Zheng, L. Hoang, C. Wang, Nafisah, C. Joseph, W. Zhang, J. Xu, Z. Li, I. Rajcan, Joint mapping and allele mining of the rolled leaf trait in rice (*Oryza sativa* L.), PLoS ONE 11 (2016) e0158246.
[44] R. Kooke, W. Kruijer, R. Bours, F. Becker, A. Kuhn, H. van de Geest, J. Buntjer, T. Doeswijk, J. Guerra, H. Bouwmeester, D. Vreugdenhil, J.J.B. Keurentjes, Genome-wide association mapping and genomic prediction elucidate the genetic architecture of morphological traits in *Arabidopsis*, Plant Physiol. 170 (2016) 2187–2203.
[45] H. Zhai, Z. Feng, J. Li, X. Liu, S. Xiao, Z. Ni, Q. Sun, QTL analysis of spike morphological traits and plant height in winter wheat (*Triticum aestivum* L.) using a high-density SNP and SSR-based linkage map, Front. Plant Sci. 7 (2016) 1617.
[46] A. Verma, M. Niranjana, S. Jha, N. Mallick, P. Agarwal, QTL detection and putative candidate gene prediction for leaf rolling under moisture stress condition in wheat, Sci. Rep. 10 (2020) 18696.
[47] S.A. Boden, C. Cavanagh, B.R. Cullis, K. Ramm, J. Greenwood, E. Jean Finnegan, B. Trevaskis, S.M. Swain, *Ppd-1* is a key regulator of inflorescence architecture and paired spikelet development in wheat, Nat. Plants 1 (2015) 1–6.
[48] L. Li, D. Li, S. Liu, X. Ma, C.R. Dietrich, H. Hu, G. Zhang, Z. Liu, J. Zheng, G. Wang, P.S. Schnable, M. Xu, The maize *glossy13* gene, cloned via BSR-Seq and Seq-walking encodes a putative ABC transporter required for the normal accumulation of epicuticular waxes, PLoS ONE 8 (2013) e82333.
[49] Y. Wang, J. Xie, H. Zhang, B. Guo, S. Ning, Y. Chen, P. Lu, Q. Wu, M. Li, D. Zhang, G. Guo, Y. Zhang, D. Liu, S. Zou, J. Tang, H. Zhao, X. Wang, J. Li, W. Yang, T. Cao, G. Yin, Z. Liu, Mapping stripe rust resistance gene *YrZH22* in Chinese wheat cultivar Zhoumai 22 by bulked segregant RNA-Seq (BSR-Seq) and comparative genomics analyses, Theor. Appl. Genet. 130 (2017) 2191–2201.
[50] Z. Huang, G. Peng, X. Liu, A. Deora, K.C. Falk, B.D. Gossen, M.R. McDonald, F. Yu, Fine mapping of a clubroot resistance gene in Chinese cabbage using SNP markers identified from bulked segregant RNA sequencing, Front. Plant Sci. 8 (2017) 1448.
[51] J. Song, Z. Li, Z. Liu, Y. Guo, L.J. Qiu, Next-generation sequencing from bulked-segregant analysis accelerates the simultaneous identification of two qualitative genes in soybean, Front. Plant Sci. 8 (2017) 919.
[52] A.C. Mallory, B.J. Reinhart, M.W. Jones-Rhoades, G. Tang, P.D. Zamore, M.K. Barton, D.P. Bartel, MicroRNA control of *PHABULOSA* in leaf development: importance of pairing to the microRNA 5' region, EMBO J. 23 (2004) 3356–3364.
[53] P. Merelo, E.B. Paredes, M.G. Heisler, S. Wenkel, The shady side of leaf development: the role of the *REVOLUTA*/*KANADI1* module in leaf patterning and auxin-mediated growth promotion, Curr. Opin. Plant Biol. 35 (2017) 111–116.
[54] S.K. Floyd, C.S. Zalewski, J.L. Bowman, Evolution of class III homeodomain-leucine zipper genes in streptophytes, Genetics 173 (2006) 373–388.
[55] W. Chen, Z. Cheng, L. Liu, M. Wang, X. You, J. Wang, F. Zhang, C. Zhou, Z. Zhang, H. Zhang, *Small Grain and Dwarf 2*, encoding an HD-Zip II family transcription factor, regulates plant development by modulating gibberellin biosynthesis in rice, Plant Sci. 288 (2019) 110208.
[56] J. Wei, H. Choi, P. Jin, Y. Wu, J. Yoon, Y. Lee, T. Quan, G. An, GL2-type homeobox gene *Roc4* in rice promotes flowering time preferentially under long days by repressing *Ghd7*, Plant Sci. 252 (2016) 133–143.